

Fast and compact multichannel photon coincidence unit for quantum information processing

Sascha Gaertner^{a)} and Harald Weinfurter

Sektion Physik, Ludwig-Maximilians-Universität, 80799 München, Germany and Max-Planck-Institut für Quantenoptik, 85748 Garching, Germany

Christian Kurtsiefer

Department of Physics, National University of Singapore, 117542 Singapore, Singapore

(Received 1 March 2005; accepted 11 November 2005; published online 21 December 2005)

We present a fast and compact multichannel coincidence unit to count all possible single and coincidence detection events in an experiment with eight single-photon detectors at once. Using high-speed electronics and a microcontroller, this device is able to process up to 800 000 events/s. The coincidence window can be tuned within a range of 4–12 ns. The device can be easily scaled to any number of input channels and is thus ideally suited for efficient multiphoton quantum information processing. © 2005 American Institute of Physics. [DOI: 10.1063/1.2149007]

I. INTRODUCTION

Advanced multiparty quantum communication^{1–6} and particularly all-optical quantum computation^{7,8} require the efficient and simultaneous recording of different multiphoton coincidence detection events. Conventional electronics for the analysis of coincidence detection events, usually consisting of a combination of logical AND gates, can be used to register only a few preselected coincidence combinations simultaneously. For the rapidly increasing number of possible coincidences between more and more detectors, extensive wiring to a rapidly increasing number of logic units becomes necessary. One has thus to compromise between the complexity of the electronics and the required measurement time, and sometimes indeed repeat measurement runs for recording different sets of coincidences.

In this article we describe a compact and fast multichannel photon coincidence unit developed to register all possible coincidence events between eight detectors simultaneously. The unit achieves this feat efficiently by recording the status of all input channels and uses this data for further numerical processing. The principle can be easily scaled to any number of input channels, thus avoiding the exponential increase of the detection logic complexity. The efficient operation and the features of this model are experimentally demonstrated based on the data obtained in a typical multiphoton experiment using pulsed parametric down-conversion.

The article is organized as follows. In Sec. II we explain the basic principle of the device. In Sec. III we present the realization for recording coincidences from eight detector channels and describe in Sec. IV the operation and performance of the coincidence unit. Its application for the analysis of multidetection events in an experimental environment, typical for quantum communication, is discussed in Sec. V.

^{a)}Electronic mail: s.gaertner@mpq.mpg.de

II. THEORY OF OPERATION

In a specific time interval n single-photon detectors are in one out of 2^n possible states representing all possible single and coincidence detection events. Each of these states can be treated as a single n -bit pattern. To acquire all possible coincidence events at once, this n -bit pattern has to be captured correctly and then processed. One possibility is to save each sampled n -bit pattern one after the other. This scheme would be mainly limited by the recording rate of the storage medium (e.g., hard disk). Another possibility is to perform an immediate histogramming as a preprocessing step for a given integration time. This is of advantage if there is no special interest in recording the sequence of individual events.

The basic operation principle of the eight-channel coincidence counter is shown in Fig. 1. Eight inputs are combined to an 8 bit pattern, which is captured after an initial event recognition (OR), and then buffered by a first-in-first-out (FIFO) memory for interpretation by the microcontroller. In a captured code word, each bit corresponds to a particular detector state, therefore any possible combination of eight detectors showing a coincidence event corresponds to an 8 bit pattern, leading to 256 possible patterns. The “0” code word does not represent any detector event and is used to indicate an empty FIFO buffer. For histogramming, we use a microcontroller which interprets the 8 bit pattern as an index for a counter array in the onboard random access memory (RAM), and increments the according content in a single step. This is a very efficient operation, which can be performed even on a moderate speed controller with sufficient throughput. Still, to avoid unnecessary dead time of the system, we use a FIFO buffer for the input data to decouple the primary event flow from the histogramming cycle. After an appropriate integration time, the histogram counter array is read by a host computer. From these data, the rate of every possible coincidence event can be extracted after little post-processing.

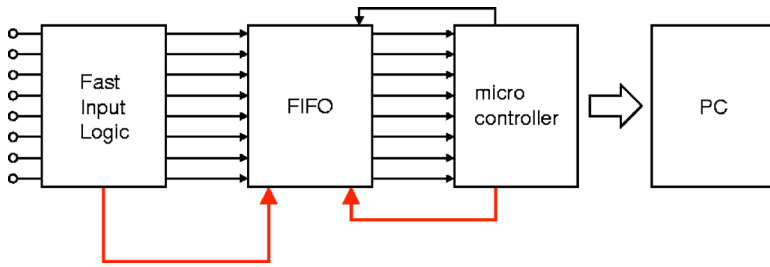


FIG. 1. (Color online) Scheme of the eight-channel coincidence unit. The device can be grouped into three different parts: A first fast part for coincidence detection and event capturing, followed by a FIFO to buffer the 8 bit patterns, and a third, slower part, containing the microcontroller for histogramming. The unit is connected via a serial interface to a personal computer (PC) for final data processing.

III. REALIZATION OF THE DEVICE

For the fast primary signal processing, the circuit was implemented in fast emitter-coupled logic (ECL) technology, and careful RF layout techniques were necessary using a four-layer printed circuit board. A simplified circuit diagram of the eight-channel coincidence unit is shown in Fig. 2.

From each avalanche photodiode detector, we receive nuclear instrumentation module (NIM) compatible signals. In the coincidence unit a first level shift from NIM to ECL and signal regeneration is performed with a MC100E416. An OR gate is used to derive a trigger signal (4OR) from the eight input lines to initiate pattern sampling into an 8 bit latch (MC10H603) after a time defined by an adjustable one shot (P1). The eight-channel OR gate is implemented by chaining four quad-input-OR/NOR gates (MC10E101). This also allows to recognize an external veto signal by hardware with only little propagation delay penalty. The latch transfers the ECL signals into standard transistor-transistor logic (TTL) levels and holds the 8 bit pattern for capturing by the slower FIFO chip (CY7C4211). The complete timing sequence is asynchronously locked to the initial trigger event using adjustable one shots, which are based on a high-speed flip-flop (MC100EL31) and have adjustment ranges from 1 to 20 ns. In order to ensure transfer from the initial latch

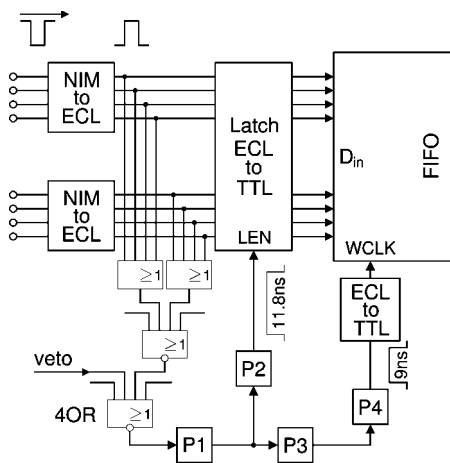


FIG. 2. Simplified circuit diagram of the fast part of the coincidence unit, relevant for the coincidence detection. The left side shows the eight input channels, for the eight detector signals (NIM), we start off with. The eight detector pulses are first turned into ECL pulses allowing fast signal processing. The whole signal processing is triggered by the output signal of an eight-channel OR gate, indicating a detection event, which is captured by an 8 bit latch. P1–P4 denote four adjustable one shots, which are used to guarantee the exact timing sequence. After the correct event recognition, the data byte representing all possible single and coincidence events is written into a FIFO buffer for further processing.

into the FIFO, a timing sequence shown in Fig. 3 is used, which is explained in detail in the next section.

The depth of the FIFO is chosen to be 512 bit, so that for primary event rates of up to 800 000 events/s, a read latency of about 640 μ s can be allowed, which can be easily accomplished with the chosen moderate speed microcontroller.

On the output side of the FIFO, signals are conditioned such that the microcontroller (MEGA332)⁹ can load the 8 bit pattern with an efficient polling scheme, to keep both hardware and processing software simple. Eight AND gates tie the output of the FIFO to 0 if the FIFO chip is empty, so that no physically meaningful 8 bit pattern is transferred in this case. An octal buffer (74HC541) and simple address decoding is used to gate the flow to the microcontroller bus. The FIFO output is represented by a single 1 byte location in the CPU address space.

Additional timing logic is necessary to accurately define an integration time window. This task is performed with an onboard time processing unit (TPU),¹⁰ which can be programmed to generate an output pulse of any desired length from a few 100 μ s to seconds, addressing the reset function of the FIFO. At the beginning of each event sampling period, the FIFO reset is asserted, leading to a reset of the device. At the end of the chosen integration time the timer interrupt of the TPU causes an absolute uncertainty of the integration time window. Since usual measurement times are above 1 s, and the timing uncertainty is on the order of a few microseconds, this tiny error on the integration time usually can be neglected. If desired, a simple way to overcome this uncertainty is to use an output pulse of the TPU as veto signal.

The histogramming algorithm implemented in the microcontroller allows an average processing time of 1.2 μ s per event reading. The hole polling and histogramming core code, together with some command interpretation and output routines via a serial (RS232) interface and interrupt routines for timing, are stored in an onboard electrically erasable programmable read-only memory (EEPROM). The only communication with the host personal computer (PC) is an initialization, together with a parameter transfer at the beginning, and a data transfer of the 256 histogram results at the end of a sampling period.

The whole high-speed signal processing together with the FIFO, the control logic, and the output logic was realized on a single circuit board, interfacing to a commercial 68332-based microcontroller. Typical power consumption is dominated by the ECL components, leading to 3.75 W at -5 V and 0.54 W at $+5$ V, respectively.

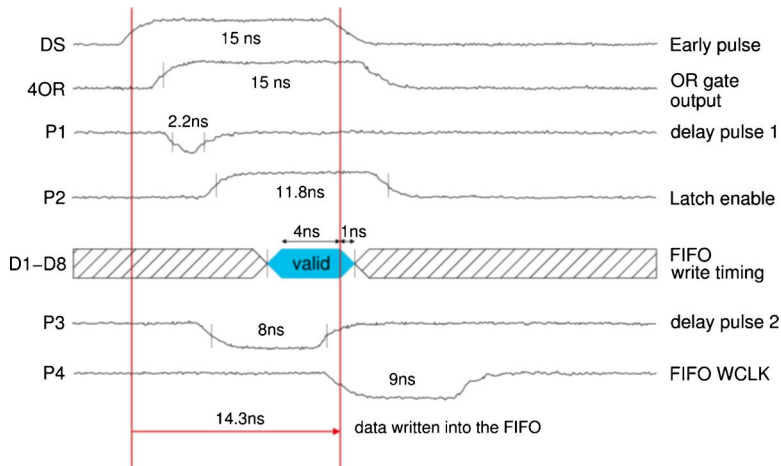


FIG. 3. (Color online) Fast side timing of the coincidence unit. The coincidence registration is initiated by a detection signal, which is denoted by DS. The output of the last OR gate is labeled by 4OR. The output signals of the four one shots providing the correct timing sequence are labeled by P1 to P4. The 8 bit pattern is written into the FIFO on the rising edge of the WCLK signal (inverted and level-shifted P4 signal).

IV. OPERATION OF THE DEVICE

In the actual implementation the detector signals follow the NIM amplitude specification, where the detection event time is defined by the leading edge of the pulse. This primary pulse shape and length (15 ns) is formed in the detector modules.

Figure 3 shows the measured timing sequence on the fast side to write the 8 bit pattern into the FIFO chip, following a single detection signal (DS) which initiates the complete data processing. The total propagation through the initial OR gate chain is 0.8–2.0 ns, resulting from the specified propagation delay of each individual gate. The output of the OR chain triggers the first one shot P1 creating a negative pulse with a duration of about 2.2 ns. The rising edge of this pulse is used to trigger a second one shot, P2, generating an 11.8-ns-long pulse to latch the detector input pattern. This pulse length was chosen to allow a sufficient setup and hold time for the transfer of the 8 bit pattern into the FIFO. To initiate this transfer, a series of two more one shots is used to drive the write clock signal (WCLK), fulfilling the setup and hold timing requirements of the FIFO chip. The theoretical total average time after which the input data can be written into the FIFO chip, resulting from the specified minimal and maximal propagation delays of each individual ECL logic component, the adjusted pulse length of the one shot P1, and an estimated signal transmission propagation delay time of

0.7 ns for the latch enable signal and the specified data setup time of the FIFO, is about 12.78 ns and cannot get smaller than 11.58 ns. The lower bound is obtained for a minimal delay pulse length of 1 ns for P1. In the present configuration (Fig. 3) the measured overall processing time of about 14 ns results mainly from the pulse length adjustment of P3.

As the readout from the FIFO is performed with a relatively low speed microcontroller, timing requirements are much more relaxed. Output flow control signals required by the FIFO are derived from the address bus signal A5 and CS10/RD via simple NOR gates, where CS10 is a custom programmable chip select output of the microcontroller, and a low on RD signals a read operation.

A. Coincidence window

One of the most important properties of the device presented is the time window in which multiple detection events are identified as coincidences. To guarantee that photo detection events caused by two consecutive laser pulses are not identified as coincidences, the coincidence window must be smaller than the repetition rate (82 MHz) of the mode-locked Ti:Sapphire laser, corresponding to a pulse distance of 12.2 ns, typically used in pulsed multiphoton experiments.

The coincidence window was measured by observing pair coincidences of an original detector signal with a delayed copy of it. We found coincidences for delays ranging from $t_{w1}=5.55$ ns to $t_{w2}=6.25$ ns, leading to an average value of $t_w=5.9$ ns. To understand how the coincidence window is defined by circuit properties, and how it can be adjusted, analysis of signal propagation has to be carried out. All detector pulses propagating to the latch chip are counted as a coincidence, if the input lines are in an active state when the latch is enabled (LEN) by the second one shot (P2). Timing details are shown in Figs. 3 and 4.

The width of the coincidence window following the first detection event can be expressed as

$$t_w = t_{d1} + t_{d2} + t_{p1} + t_{d3} + t_{d4} + t_l, \quad (1)$$

with the following parameters:

- t_{d1} : delay time through the four OR/NOR-gates,
- t_{d2} : propagation delay time of one shot P1,
- t_{p1} : pulse length of one shot P1,

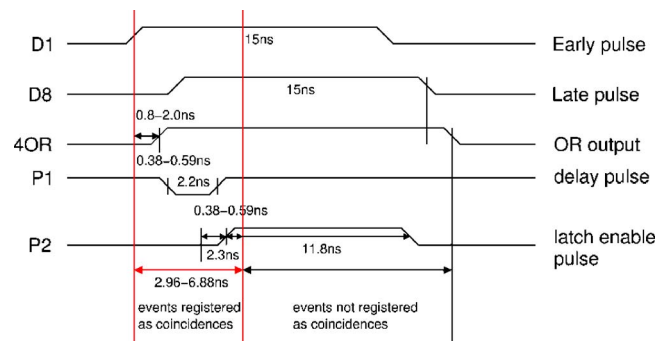


FIG. 4. (Color online) Timing of the coincidence window. D1 and D8 denote two exemplary detector signals. The output pulse of the last OR gate is labeled by 4OR. P1 and P2 denote the output pulses of the first two one shots, allowing to tune the coincidence window. The theoretical expected average coincidence window with the present setup is $t_w \approx 4.92$ ns.

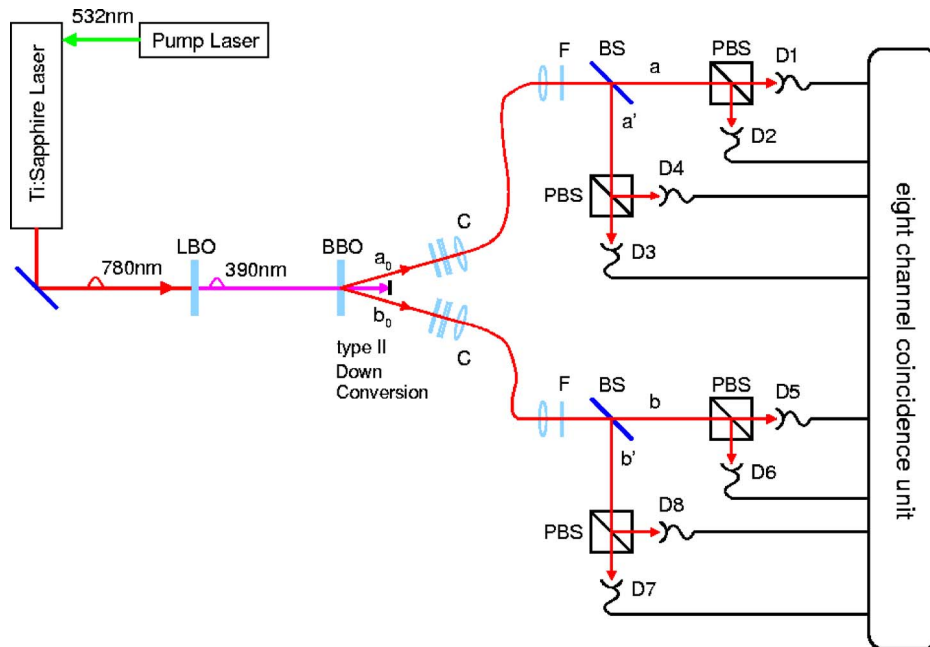


FIG. 5. (Color online) Experimental setup to demonstrate the operation of the multichannel coincidence counter (LBO: lithium triborate crystal, BBO: beta barium borate crystal, C: fiber coupler, F: narrow bandwidth filter $\Delta\lambda=3$ nm, BS: beam splitter, PBS: polarizing beam splitter, and D1-D8: single-photon detectors). In different orders n of the parametric down-conversion process n photon pairs are created. The multiphoton emission is analyzed with the eight-channel coincidence counter presented here.

- t_{d3} : propagation delay time of one shot P2,
- t_{d4} : LEN signal transmission delay time, and
- t_i : setup time and hold time of the latch.

Since there is an uncertainty, resulting mainly from the timing requirements of the latch, the time period after which the data is finally latched and due to mismatches in the propagation delays of the OR gate chain and the one shots, there is a minimal and maximal coincidence window to be expected. According to the manufacturer specifications the propagation delay times t_{d1} for each OR gate are ranging from 0.2 to 0.5 ns and the propagation delay times t_{d2} and t_{d3} of the one shots P1 and P2 are specified within 0.38–0.59 ns. Using $t_{p1}=2.2$ ns, $t_{d4}=0.7$ ns, a setup time of -1.5 ns, and a hold time of 0.8 ns for the latch, the coincidence windows should range between

$$t_w^{\min} = (0.8 + 0.38 + 2.2 + 0.38 + 0.70 - 1.5) \text{ ns} = 2.96 \text{ ns},$$

$$t_w^{\max} = (2.0 + 0.59 + 2.2 + 0.59 + 0.70 + 0.8) \text{ ns} = 6.88 \text{ ns}.$$

The estimated bounds are in good agreement with the measured average value of $t_w=5.9$ ns. The coincidence window can be varied within some limits by changing the pulse length t_{p1} of the first one shot P1. Because the pulse length of one shot P1 cannot get below 1 ns, the shortest coincidence window achievable with the current setup is about 3.72 ns.

To overcome this limit, we would have to introduce a delay for the detector signals propagating into the capture latch and to use a fast latch, then allowing for coincidence time windows only limited by timing jitter, signal path mismatches, and the timing conditions of the latch. Assuming detector time jitter of about 1 ns, signal path mismatches below 0.5 ns, and a latch with a setup time and hold time below 0.5 ns, the lower bound for such a coincidence time window would be about 2 ns. Such a shortening of the coincidence window would help reducing the registration of accidental coincidences, which might be of interest in quantum

optical experiments with continuous wave (cw) pump sources but is of no significant concern in experiments where pulsed sources are used.

B. Data processing

The largest mean event rate digestable by the unit is given by the processing time of the processor for one histogramming cycle. We have measured a processing time of 1.2 μs , corresponding to a maximal processing rate of about 800 000 events/s. Since the whole initial coincidence capture and FIFO transfer takes about 14 ns we can only detect those events which are created by every second laser pulse.

To correctly identify all possible coincidences and primary events from an observed coincidence pattern, we have to perform a postprocessing on the raw histogram data. For example, a bit pattern equal to “00101011” is not only labeling a fourfold coincidence, it also contains a number of three- and twofold coincidences and of course four single events. The postprocessing algorithm is performed after detection in the host PC.

V. EXPERIMENTAL RESULTS

Some of the basic properties of the coincidence unit, such as the coincidence time window and proper identification of multidetector events, were verified with well-defined test signals.

To demonstrate the powerful operation of the coincidence counter in a realistic experiment, we present an analysis of multiphoton coincidence events obtained from pulsed parametric down-conversion. A more detailed characterization of the pulsed parametric down-conversion source will be published elsewhere.¹¹

The experimental setup is shown in Fig. 5. We use a Ti:Sapphire laser emitting pulses of light at a central wavelength of $\lambda=780$ nm with a duration of about 180 fs at a repetition rate of 82 MHz. This radiation is frequency

doubled in a lithium triborate (LBO) crystal, and the UV light is then used to pump a 2-mm-thick type-II cut beta barium borate (BBO) crystal. In the first-order process of type-II parametric down-conversion, a pump photon is split into two highly correlated photons with different polarizations.¹² Generally processes of the order n lead to the creation of n correlated photon pairs, or $2n$ photons. The correlated photons are collected into two single mode fibers. To analyze the multiphoton emission, we split the photons in each fiber at a 50/50 optical beam splitter (BS) and perform a polarization analysis in each of the four output modes a , a' , b , and b' behind the BS. For this purpose, we use polarizing beam splitter (PBS) followed by silicon avalanche photodiodes (Si-APD) capable to register single photons. The output signals of these eight photodetectors denoted by D1-D8 are then analyzed with the device presented above.

The $2n$ photon state obtained from type-II parametric down-conversion is given by^{11,13}

$$|\Psi_{DC}^n\rangle = \frac{1}{\sqrt{n+1}} \frac{1}{n!} (a_{0H}^\dagger b_{0V}^\dagger - a_{0V}^\dagger b_{0H}^\dagger)^n |0\rangle, \quad (2)$$

where a_{0H}^\dagger (a_{0V}^\dagger) describes the creation of a horizontally (vertically) polarized photon in mode a_0 and so on. In the first-order process ($n=1$) a two-photon polarization entangled state can be obtained,¹² often used for the demonstration of quantum communication between two parties, such as quantum dense coding¹⁴ or quantum teleportation.¹⁵ The second order ($n=2$) describes the creation of four photons.¹⁶ Restricting this state to contributions with detectable fourfold coincidences in modes a , a' , b , and b' leads to the following normalized four-photon state behind the two beam splitters:

$$\begin{aligned} |\Psi^4\rangle = \frac{1}{\sqrt{6}} & \left[|H_a H_{a'} V_b V_{b'}\rangle + |V_a V_{a'} H_b H_{b'}\rangle \right. \\ & - \frac{1}{2} (|H_a V_{a'} H_b V_{b'}\rangle + |H_{a'} V_{a'} H_b V_{b'}\rangle) \\ & + |H_a V_a H_b V_{b'}\rangle + |V_a H_{a'} H_b V_{b'}\rangle + |H_a V_{a'} H_{b'} V_{b'}\rangle \\ & + |H_{a'} V_{a'} H_{b'} V_{b'}\rangle + |H_a V_a H_{b'} V_{b'}\rangle \\ & + |V_a H_{a'} H_{b'} V_{b'}\rangle + |H_a V_{a'} H_b V_b\rangle + |H_{a'} V_{a'} H_b V_b\rangle \\ & + |H_a V_a H_b V_b\rangle + |V_a H_{a'} H_b V_b\rangle + |H_a V_{a'} V_b H_{b'}\rangle \\ & + |H_{a'} V_{a'} V_b H_{b'}\rangle + |H_a V_a V_b H_{b'}\rangle \\ & \left. + |V_a H_{a'} V_b H_{b'}\rangle \right]. \quad (3) \end{aligned}$$

This state contains 18 terms, which are a subset of all four-photon terms described by (2) for $n=2$. A record of all possible fourfold coincidences between the eight detectors is shown in Fig. 6. Since the eight single-photon detectors exhibit different detection efficiencies due to production tolerances, the four-photon coincidence rates presented here are corrected for the separately calibrated efficiencies, without changing the overall detection rate.

As expected, the measurement shows significant population of 18 different fourfold coincidences as described by (3). The nonvanishing event rate on the other remaining fourfold

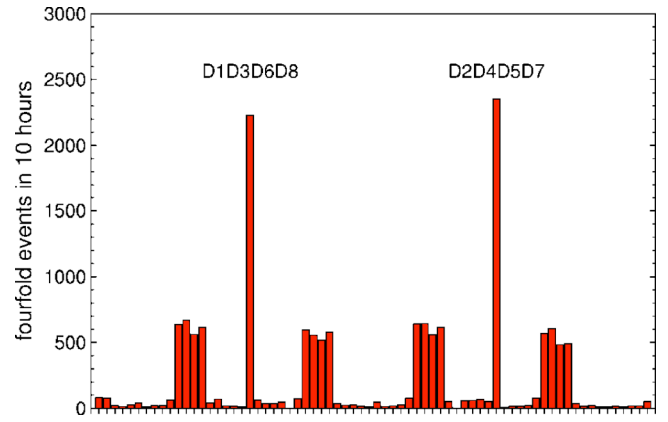


FIG. 6. (Color online) All possible 70 fourfold coincidences between the eight detectors D1-D8. The theory predicts the registration of 18 different fourfold coincidences with two different detection probabilities. Labeled are the two fourfold coincidences corresponding to the first two terms in Eq. (3). The registration of this coincidences should be four times higher than the registration of all other events.

detector combinations is mainly resulting from the experimentally achieved nonperfect four-photon correlations. This measurement demonstrates the efficient detection of all possible different fourfold coincidences in a quantum optical experiment with eight detectors.

To demonstrate that the device is able to process all possible single and coincidence events at once, the complete emission of the parametric down-conversion can be analyzed. Generally, there are m different x -fold coincidences between n detectors:

$$m = \frac{n!}{[(n-x)! \cdot x!]} \quad (4)$$

To show the correct registration of all single and coincidence events, all single count rates and all multiphoton coincidence events of the same type can be summed up and compared with the theory. The sum N of all experimentally observed x -fold coincidences, together with the theoretical prediction, is shown in Fig. 7. The overall measurement time for the analysis of the emission of the pulsed parametric down-conversion was 60 h. The complete measurement was performed without interruption and the total number of acquisitions was about 4.3×10^{10} . For the evaluation the raw data directly obtained from the experiment were used. As one can see, the presented eight-channel coincidence unit is capable to register all 255 possible single and coincidence events at once and to cover a range of ten orders of magnitude in count rates.

VI. DISCUSSION AND OUTLOOK

The experimental results shown here clearly demonstrate the high performance of the multichannel coincidence unit in multiphoton experiments.

Meanwhile the presented eight-channel coincidence counter was already used for the realization of several experiments. The device was used to analyze different three- and four-photon polarization entangled states,¹⁷⁻¹⁹ which form the basis for multiparty quantum communication, to

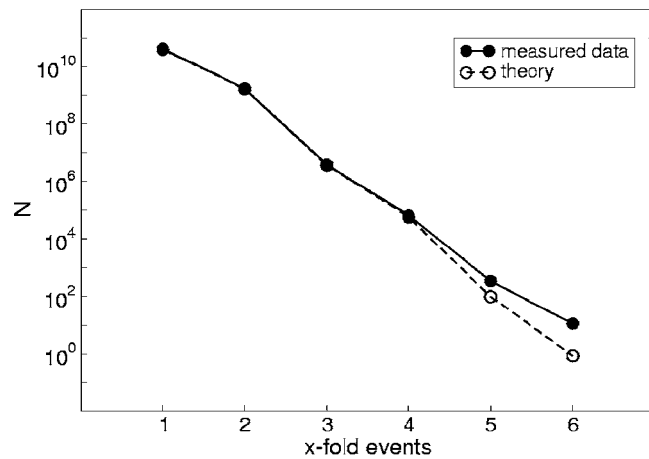


FIG. 7. Analysis of the multiphoton emission of the pulsed parametric down-conversion source. Shown is, on logarithmic scale, the sum N of all m possible single detection events and x -fold coincidence detection events registered in an overall measurement time of 60 h. The experimental results are compared with the theory. This measurement indicates that the developed multichannel coincidence unit is able to process all possible 255 different detection events at the same time, and therefore clearly demonstrates the powerful and efficient operation of this type of instrument.

study multiphoton entanglement^{20,21} and to demonstrate decoherence-free quantum communication between two parties.²²

We are convinced that the efficient event detection with the presented compact multichannel coincidence unit, or similar devices based on the same principle, will strongly influence future development of quantum communication because it enables the experimental demonstration of multiparty quantum communication protocols with more than two photons, such as quantum secret sharing,²³ quantum telecloning,⁶ or other quantum communication schemes.

Moreover, such a detection unit will be essential for the realization of linear optics quantum computation,^{7,8} which requires the simultaneous detection and registration of a huge number of photons.

ACKNOWLEDGMENTS

The authors want to thank H. D. Paul from MCT for useful discussions about the MEGA332. This work was supported by the EU-Projects QuComm (IST-FET-10033) and RamboQ (IST-FET-38864).

- ¹ A. Karlsson and M. Bourennane, Phys. Rev. A **58**, 4394 (1998).
- ² B.-S. Shi and A. Tomita, Phys. Lett. A **296**, 161 (2002).
- ³ W. Dür and J. I. Cirac, J. Mod. Opt. **47**, 247 (2000).
- ⁴ M. Hillery, V. Bužek, and A. Berthiaume, Phys. Rev. A **59**, 1829 (1999).
- ⁵ R. Cleve, D. Gottesmann, and H.-K. Lo, Phys. Rev. Lett. **83**, 648 (1999).
- ⁶ M. Muraio, D. Jonathan, M. B. Plenio, and V. Vedral, Phys. Rev. A **59**, 156 (1999).
- ⁷ E. Knill, R. Laflamme, and G. J. Milburn, Nature (London) **409**, 46 (2001).
- ⁸ M. Koashi, T. Yamamoto, and N. Imoto, Phys. Rev. A **63**, 030301 (2001).
- ⁹ MEGA332 is a single board computer based on the MC68332 from Motorola, <http://www.mct.net>
- ¹⁰ Motorola Inc., TPU Time Processing Unit, Reference Manual, Motorola Inc. (1996).
- ¹¹ S. Gaertner, C. Kurtsiefer, and H. Weinfurter (to be published).
- ¹² P. G. Kwiat, K. Mattle, H. Weinfurter, A. Zeilinger, A. V. Sergienko, and Y. Shi, Phys. Rev. Lett. **75**, 4337 (1995).
- ¹³ G. A. Durkin, C. Simon, and D. Bouwmeester, Phys. Rev. Lett. **88**, 187902 (2002).
- ¹⁴ K. Mattle, H. Weinfurter, P. G. Kwiat, and A. Zeilinger, Phys. Rev. Lett. **76**, 4656 (1996).
- ¹⁵ D. Bouwmeester, J. W. Pan, K. Mattle, M. Eibl, H. Weinfurter, and A. Zeilinger, Nature (London) **390**, 575 (1997).
- ¹⁶ H. Weinfurter and M. Zukowski, Phys. Rev. A **64**, 010102 (2001).
- ¹⁷ M. Eibl, S. Gaertner, M. Bourennane, C. Kurtsiefer, H. Weinfurter, and M. Zukowski, Phys. Rev. Lett. **90**, 200403 (2003).
- ¹⁸ S. Gaertner, M. Bourennane, M. Eibl, C. Kurtsiefer, and H. Weinfurter, Appl. Phys. B: Lasers Opt. **77**, 803 (2003).
- ¹⁹ M. Eibl, N. Kiesel, M. Bourennane, C. Kurtsiefer, and H. Weinfurter, Phys. Rev. Lett. **92**, 077901 (2004).
- ²⁰ M. Bourennane *et al.*, Phys. Rev. Lett. **92**, 087902 (2004).
- ²¹ M. Bourennane, M. Eibl, N. Kiesel, S. Gaertner, C. Kurtsiefer, and H. Weinfurter, Phys. Rev. Lett. (submitted).
- ²² M. Bourennane, M. Eibl, S. Gaertner, C. Kurtsiefer, A. Cabello, and H. Weinfurter, Phys. Rev. Lett. **92**, 107901 (2004).
- ²³ S. Gaertner, C. Kurtsiefer, and H. Weinfurter (to be published).